

# MICROSTRUCTURE AND TEXTURE FORMATION OF THIN HOT ROLLED STEEL STRIPS

Roumen Petrov<sup>\*</sup>, Leo Kestens<sup>\*</sup>, Rafael Colás<sup>\*\*</sup>, and Yvan Houbaert<sup>\*</sup>

<sup>\*</sup> Department of Metallurgy and Materials Science, Ghent University, Technologiepark 903, B-9052, Zwijnaarde (Gent), Belgium

<sup>\*\*</sup> Facultad de Ingeniería Mecánica y Eléctrica, Universidad Autónoma de Nuevo León, A.P. 149-F, 66451 San Nicolás de los Garza, N.L., Mexico

## SUMMARY

Plain carbon steel and an Nb containing steel were directly hot rolled, after being cast into slabs of around 50 mm in thickness, in an industrial, six-stand continuous rolling mill to a final thickness that varied from 2.7 to 1.06 mm. The microstructure and texture of the thin strips was studied by means of classical metallography and orientation image microscopy (OIM) in the middle thickness of the strips.

It was found that the average grain diameter of plain carbon hot rolled strips varies from 7 to 10  $\mu\text{m}$  and depends on the total amount of reduction, whereas for the Nb steel it decreases to 3.6  $\mu\text{m}$ .

The middle thickness texture of the Nb steel is typical transformation texture originating from strained austenite, whereas the type and intensity of the ferrite texture in the strips depends on the thermo-mechanical history of the steel strip. The increase of strain at elevated temperatures leads to intensification of the ferrite texture and all typical transformation components from the recrystallized austenite phase are presented. When the strain at elevated temperature is low the texture is weak and additional transformation components emerging from deformed austenite are dominant. The data confirm that by proper control of the processing parameters it is possible to obtain thin hot rolled strips with fine grains and appropriate texture providing satisfactory levels of strength and formability.

## 1. INTRODUCTION

When the high surface quality of the thin steel strips is not of the prime importance for their application, hot rolled thin strips could be used as a viable economical alternative of cold rolled steel strips. This replacement can be more effective when mechanical properties of the hot rolled thin strips, i.e. strength, toughness and formability are high enough and are combined with low values of anisotropy. Such a combination of properties may be achieved by means of thermo-mechanical treating that results in a fine-grained microstructure with an appropriate texture.

Improvements in thin slab casting, hot direct charging together with hot rolling techniques and practices have resulted in the production at an industrial scale, of hot rolled strips of gauges thinner than 2 mm. Such processing implies that the reductions of thickness in the originally cast slab is higher than 96%. Furthermore, hot direct charging of thin cast slab does not permit the common isotropic transformations that take place in conventionally processed material<sup>1)</sup>.

The goal of the present work is to study the influence of processing parameters on the microstructure and texture of two carbon steels, one plain and the other with Nb addition, which were cast into thin slabs and hot rolled in a compact strip mill to different final thickness.

## 2. EXPERIMENTAL

Two low carbon steels, designated as A (plain carbon) and B (with higher Mn and Nb contents), were hot rolled in an industrial six-stand continuous rolling mill to different final thickness directly after being cast into slabs of around 50 mm in thickness. The chemical composition of the steels is shown in Table 1. Full details of the mill can be found elsewhere <sup>1)</sup>.

Table 1. Composition of the steels.

Steel	Chemical composition, mass.%							
	C	Mn	P	S	Si	Al	Nb	N
A	0.054	0.199	0.01	0.006	0.015	0.033	0.003	0.0043
B	0.064	0.804	0.01	0.006	0.008	0.033	0.023	0.0055

Three different rolling schedules were used with steel of composition A (identified as A1, A2 and A3), whereas only one schedule, similar to that of A2, was applied with steel B. The samples from either type of material were cut at room temperature from the coiled product. Coiling of the strips takes place at the end of the run out table. The later was equipped with a cooling system, which assure coiling temperature below 650°C. Some parameters of the rolling schedules – rolling temperature, thickness and reduction at each stand are shown in Fig.1.

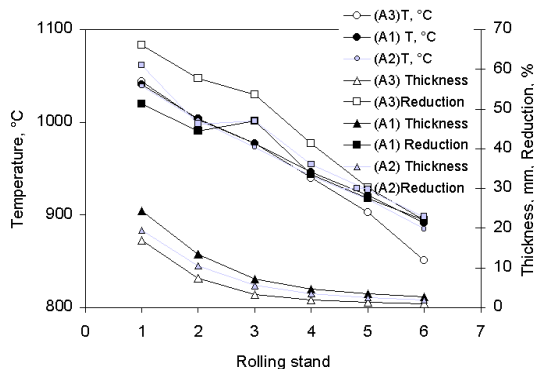


Fig.1 Data of the rolling schedules (rolling temperature, thickness and reduction) for strips A1, A2 and A3. The  $Ar_3$  temperature (860°C) is the dashed line.

The value of critical temperatures  $A_1=718^\circ\text{C}$  and  $A_3=860^\circ\text{C}$  were calculated with the equations proposed by Andrews <sup>2)</sup>. The temperature changes in the strips during rolling were predicted by computer modeling <sup>3)</sup>, as this approach allows to have an idea whether the final rolling temperature (FRT) stays within the austenite phase field or within the two phase,  $\alpha+\gamma$ , region. The values shown in Fig.1 indicate that the final rolling temperatures predicted by the model for the rolling schedules A1, A2 and B were above  $A_3$ , without entering the in-

tercritical region, but not for the thinnest sample (A3), on which the final pass may have been imparted in the intercritical region ( $T=850^\circ\text{C}$ ).

Evaluation of the forming characteristics of the hot rolled steels was carried out following the standard procedure for determination of the average value of the normal anisotropy R of the sheets, by means of tensile tests as it is reported elsewhere <sup>4,5)</sup>. The same characteristic was calculated on the base of the texture measurements using the full constraints model.

The microstructure of the samples was examined in their cross section after standard sample preparation procedure finished with 2 % nital etching. The plane for observation was perpendicular to the transverse direction of the rolled sheet. In the centre of this plane (middle thickness of the strip) were performed local microtexture measurements by means of orientation imaging microscopy (OIM). The OIM attachment was installed on a Philips XL30 ESEM with an  $\text{LaB}_6$  filament and the electron backscattering diffraction (EBSD) patterns were acquired and analysed by means of the com-

mercial TSL OIM\* software<sup>6)</sup>. The orientation data of at least 3 local measurements of each sample were summarized and further post processed by means of FHM-MTM software developed by Van Houtte<sup>7)</sup> in order to represent the texture of the strips by means of the orientation distribution functions (ODFs). Every ODF created in this way represents statistically reliable texture data.

thickness of the strips. The differences between the microstructure and grain size in the mid-thickness and in the surface layers of the strips are negligibly small and they are shown in Fig.3b.

Strong grain refinement is observed in steel B, which contains 0.023%Nb. The average grain diameter ( $D_{av}$ ) measured in this steel (cf. Fig. 3a) is 3.6  $\mu\text{m}$  that is 2.5 times

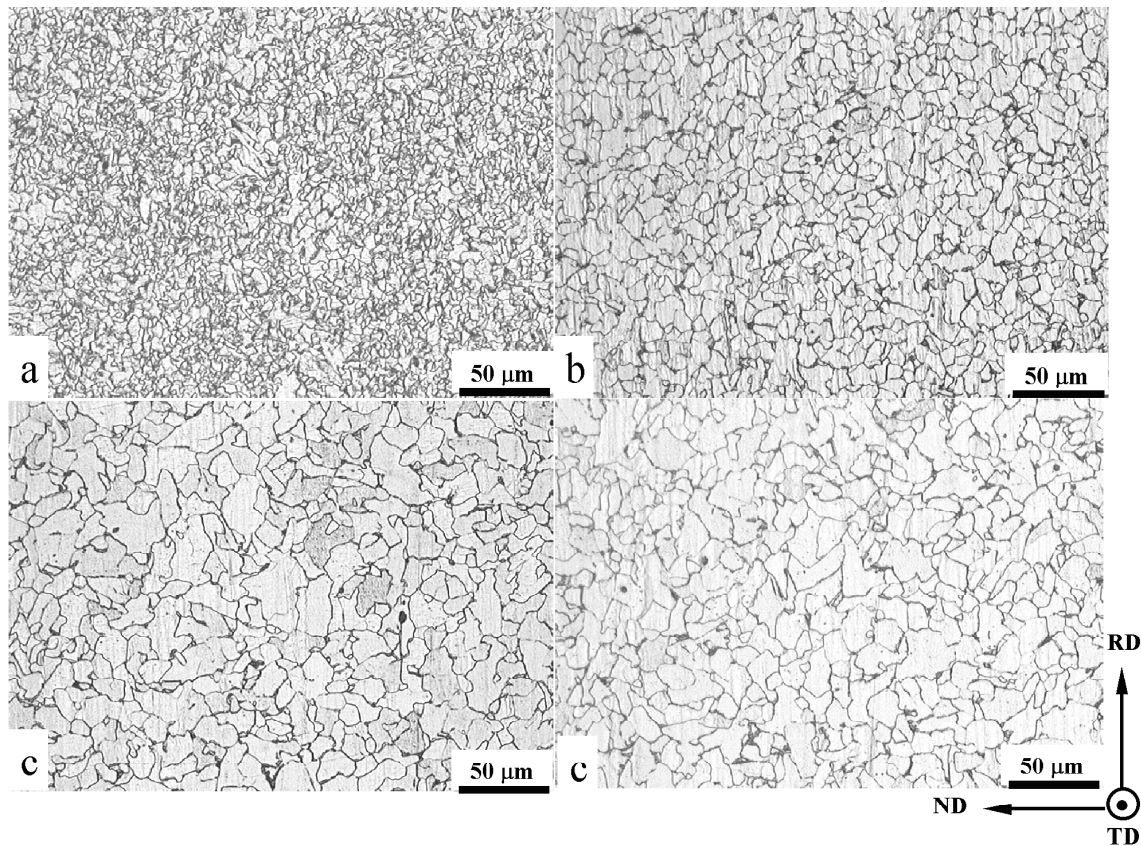


Fig.2. Microstructure of the middle thickness of the strips; (a) Steel B,  $t=2.18$  mm; (b) Steel A3,  $t=1.06$  mm; (c) Steel A2,  $t=1.92$  mm; (d) Steel A1,  $t=2.69$  mm

### 3. RESULTS AND DISCUSSION

#### 3.1. Microstructure

The microstructure observation (Fig.2a-d) displays that the average grain diameter  $D_{av}$ , which was used to define the grain size of the strips, changes significantly as a function of the chemical composition of the steel and the processing parameters. Fig.3a shows the changes in the grain diameter and the area fraction of the grains in the mid-

smaller than the average grain diameter measured in strips A1, A2 and A3 (compare the data in Fig. 3a). The grains smaller than 5 $\mu\text{m}$  include between 75% and 95% of all number of grains but cover only 30 % of the area.

The ferrite grains in plain carbon steel are larger than those in the Nb containing steel B, and their average diameter vary from 7.2  $\mu\text{m}$ , for strip A3, to 10  $\mu\text{m}$ , for strip A1. Metallographic observation did not show significant differences between the

\* TSL OIM is a trade mark of TexSem Laboratories INC., Draper, UT, USA..

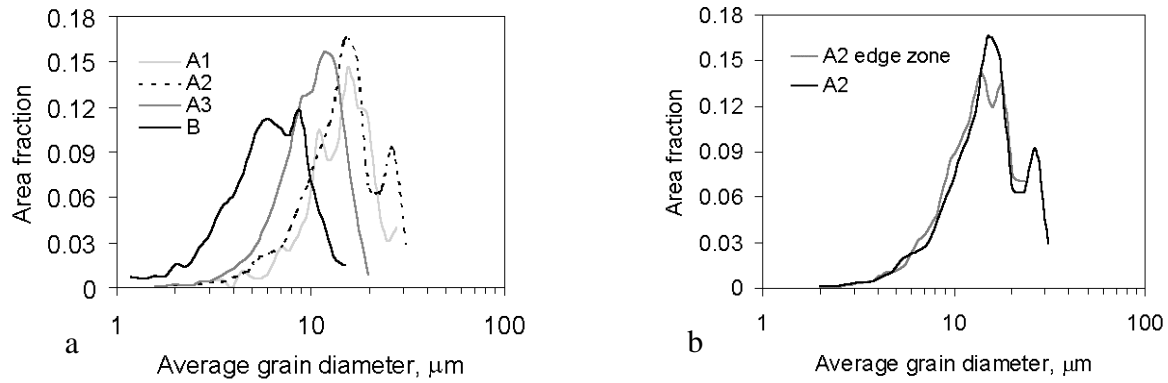


Fig.3: (a) Area fraction of the grains plotted vs. grain diameter for steels B ( $D_{av}=3.6\mu\text{m}$ ), A3 ( $D_{av}=7.2\mu\text{m}$ ) and A1 ( $D_{av}=10\mu\text{m}$ ); (b) Grain diameter measured in the center of the strip ad in the edge zone (strip A2,  $D_{av,center}=9\mu\text{m}$ ,  $D_{av,edge}=7\mu\text{m}$ ).

microstructure (grain size and shape) in the surface and in the mid-thickness of the strips (Fig.3b), but somehow, the grains close to the surface are slightly smaller in diameter than those in the mid-thickness. The grain refining effect, which was observed in the plain carbon strips, as a function of the rolling reduction, could be associated with the changes in the dislocation density of the parent austenite phase prior to transformation. An indirect proof of this assumption is the difference between the austenite grain size predicted by the computer model <sup>3)</sup> and the grains measured in the final ferrite.

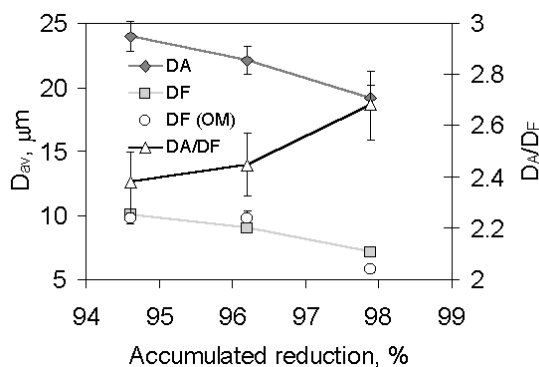


Fig.4: Changes in the average austenite grain diameter  $D_A$ <sup>3)</sup>, average ferrite grain diameter  $D_F$  and the  $D_A/D_F$  ratio as a function of the rolling reduction in the plain carbon steel strips. The white dots display the average ferrite diameter measured by the linear interception method

Fig 4 displays the ratio  $D_A/D_F$  for the strips of plain carbon steel A1, A2 and A3, where  $D_A$  is the average austenite grain diameter before the transformation predicted by the model <sup>3)</sup> and  $D_F$  is the size of the ferrite. It can be considered that with increase of this ratio more ferrite grains (with a small diameter) are nucleated from a single austenite grain, assuming that there is no grain growth during coiling. Because coiling was executed at temperatures below 650°C, such assumption seems reasonable. Therefore, the number of ferrite grains emerging from a single austenite grain will be a function only of the deformed substructure of the austenite, and can be used as a qualitative characteristic of the accumulated plastic deformation in the parent austenite prior to transformation. The data in Fig. 4 show that austenite grains of a given size produce ferrite grains of smaller size as the total accumulated strain increases, i.e. the  $D_A/D_F$  ratio increases with an increase of the rolling reduction.

### 3.2. Texture.

The texture of strip B (Fig. 5a), which was calculated on the basis of 5 different local measurements, displays two important components of ferrite that were generated from deformed austenite. The  $\{332\}\langle 113 \rangle$  ferrite texture component, which is considered as a favorable orientation from the viewpoint of drawability<sup>8,9)</sup> (high R-value)

is presented with an intensity of 2.5X. The  $\{112\}\langle 131 \rangle$  component, which also represents a transformation product from deformed austenite, appears with a maximum intensity of 3.2X. This component, together with the rotated cube that was observed with an intensity of 2 X, are considered to have a detrimental effect on the R-value<sup>9)</sup>.

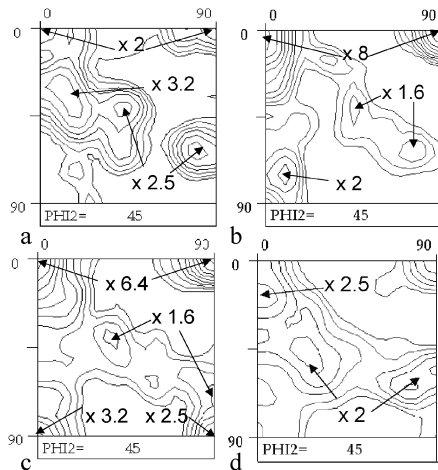


Figure 5: Mid-thickness texture of the strips (a) B,  $t=2.18\text{mm}$ ; (b) A3,  $t=1.06\text{mm}$ ; (c) A2,  $t=1.92\text{mm}$ ; (d) A1,  $t=2.69\text{mm}$

The analysis of the distribution of the texture components among grains of different size was done by calculating the ODF from grains smaller than  $3\ \mu\text{m}$  and larger than  $10\ \mu\text{m}$ , as they can be clearly discriminated in steel B. The ODF plots shown in Fig. 6c and d correspond to the smaller and larger grains shown in Fig. 6a and b, respectively. The small and large ferritic grains both display the transformation texture originating from deformed parent  $\gamma$  phase. The transformation texture components of the deformed austenite  $\{332\}\langle 113 \rangle$  (shifted to  $\{554\}\langle 225 \rangle$ ),  $\{111\}\langle 112 \rangle$  displaying an intensity of 6X and  $\{001\}\langle 010 \rangle$  with an intensity of 4 X are the strongest components in the ODF of the grains larger than  $10\ \mu\text{m}$ , whereas the  $\{001\}\langle 110 \rangle$  and  $\{110\}\langle 110 \rangle$  components appear with intensities of 3X, respectively (Fig.6 d). According to some authors<sup>9,10,11.)</sup> these texture components could emerge from either deformed or recrystallized austenite but the later is less

probable, taking into account the Nb content of steel B and the rolling parameters.

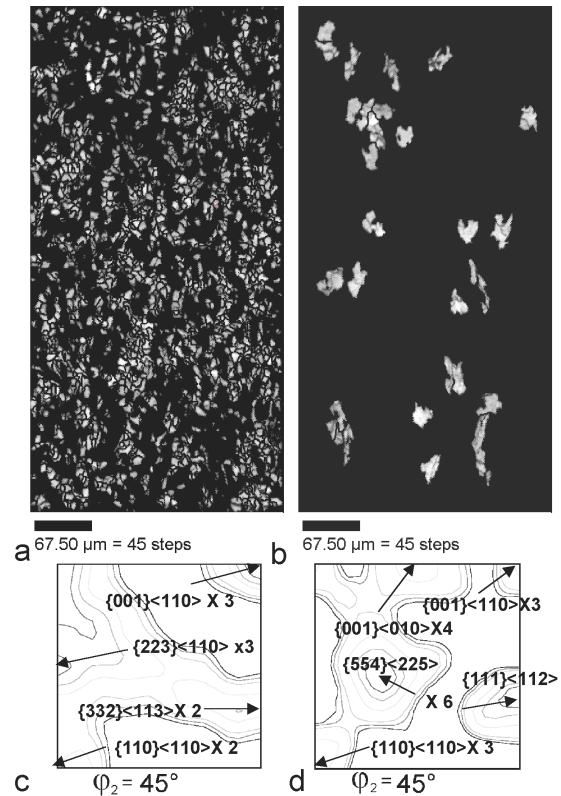


Fig.6: Image quality maps showing the grains smaller than  $3\ \mu\text{m}$  (a) and larger than  $10\ \mu\text{m}$  (b) together with the corresponding ODFs gathered from small (c) and large (d) grains

The ODF of the grains smaller than  $3\ \mu\text{m}$  (Fig. 6c) displays almost equal intensity of both ferrite texture components that could emerge from deformed austenite ( $\{223\}\langle 110 \rangle$  and  $\{332\}\langle 113 \rangle$ ) with intensity of 2~3X and from recrystallized austenite ( $\{001\}\langle 110 \rangle$  and  $\{110\}\langle 110 \rangle$ ) with intensity of 2~3X.

Considering the data of the grain size diameter and how the texture components are distributed among them it can be concluded that the strong deformed grains are among the first to transform into ferrite and hence, they have a growth advantage with respect to later transformed grains that might have emerged from the partially recrystallized austenite.

### K-S transformation products of $\gamma$ -phase with Brass, Copper and Goss orientation

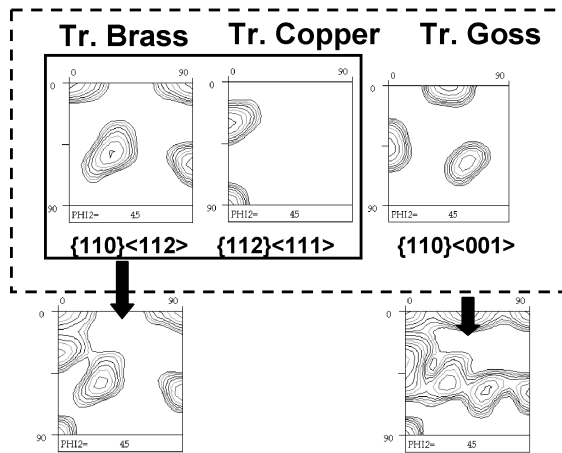


Fig.7: Modeled ferrite transformation textures obtained after  $\gamma/\alpha$  transformation of  $\gamma$  phase with (a) Brass, Copper and (b) Brass, Copper and Goss orientation

A simple modeling of ferrite transformation textures produced after  $\gamma/\alpha$  phase transformation regarding the K-S crystallographic orientation relationship (i.e. rotation of  $90^\circ$  about  $\langle 112 \rangle$  axis) is shown in Fig.7. The  $\gamma$  parent phase with Brass  $\{110\}\langle 112 \rangle$ , Copper  $\{112\}\langle 111 \rangle$  and Goss  $\{110\}\langle 001 \rangle$ , which are characteristic texture components of strained austenite orientations, gives rise after the transformation to the same transformation texture components that were observed in the industrially hot rolled thin strip B. It should be mentioned that almost exact correspondence between measured and modeled texture were found in the large ferrite grains. (Compare the textures in Fig.6d and Fig.7b.).

The textures of plain carbon steel strips are shown in Fig. 5b, c and d. In general the texture of the strips A3 and A2 differ significantly from the texture of the Nb steel, whereas the texture of strip A1 looks similar to it. The intensity of the texture increases with the increase of the total rolling reduction and the thinnest strip A3 displays the strongest texture. Two main groups of texture components are presented in the ODFs of the plain carbon steel. The first

group corresponds mainly to transformation products emerging from recrystallized austenite (i.e. rotated cube, rotated Goss and Goss). The intensity of the rotated cube component is stronger in the thinner strips A3 and A2 displaying a value of 8 and 6.4 X respectively and only 2X in the thickest strip A1. The rotated Goss and Goss components are concurrently present only in the texture of strip A2, whereas the rotated Goss component with a certain deviation from the exact position is observed also in the texture of the thinnest strip A3. The transformation components from deformed austenite are weak in the textures of the strips A3 and A2 but they are the strongest components in the texture of the strip A1 with a thickness of 2.69 mm, which displays the highest R-value.

Hence, the improvement of the R-value in the thickest strip is due to the two main reasons: (i) a general decrease of the intensity of unfavorable components and (ii) the development of the  $\{111\}\langle 112 \rangle$  texture component which has a positive effect on the deep drawability<sup>9)</sup>. The calculation of the R-values based only on the texture measurements supports this assumption (cf.Fig.9).

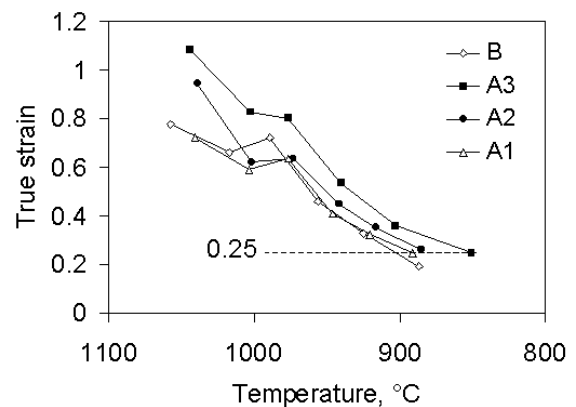


Fig.8: True strain per pass for the different strips a function of the rolling temperature

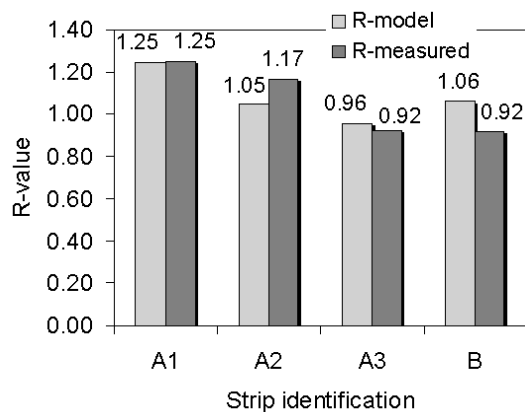


Fig.9: Measured and modeled data for the average normal anisotropy (R-value) of the strips

For better understanding the texture formation in hot rolling of thin strips, it is necessary to know also the strain distribution among the different passes. Fig. 8 displays the evolution in the reduction of the strips thickness presented by the true strain for every rolling pass. Strips A2 and A3 were subjected to higher reductions at elevated temperatures than strip A1 but in the final pass all strips received an almost identical rolling strain of 0.25. If the reduction at elevated temperatures is higher the intensity of the ferrite transformation texture from recrystallized austenite is stronger (Cf. Fig.8 and 5b, c, d), because the high temperature deformation intensifies the recrystallization of the austenite. Hence, taking into account the texture data in Fig. 5b,c,d and the data in Fig.8 it is possible to assume that recrystallization in the thickest strip A3 develops weaker than in the thinnest strips, as far as it was subjected to the lower strain. In a later stage it will be possible to employ the present data to extend the  $\gamma$ -recrystallization model<sup>3)</sup> to a fully quantitative texture dependant description

#### 4. CONCLUSIONS

The microstructure and texture of thin strips produced by hot rolling of hot charged-thin cast slabs is studied in this work. Two types of steels were studied, plain carbon steel, subjected to total hot rolling reduction of 94 to 98%, and Nb containing steel finish

rolled to a total reduction of 94%. It was found that the final grain size on hot rolled plain carbon steels ranged from 7 to 10  $\mu\text{m}$ , was dependant on the total amount of reduction during hot rolling. Significant grain refining was observed to occur in the Nb containing steel in which the average grain size was 3.6  $\mu\text{m}$ .

A low intensity transformation texture from deformed austenite was observed in the Nb containing steel, whereas the type and intensity of ferrite texture in the plain carbon steels depends on the thermo-mechanical history of the steel strip. When the reduction at elevated temperatures is higher the ferrite texture intensifies and possesses all typical transformation components from the recrystallized austenite phase. When the strain at elevated temperature is low the texture is weak and additional transformation components emerging from deformed austenite are dominant. The observed texture data of plain carbon steel are in good correlation with the results from R-value measurements.

The data confirm that by proper control of the processing parameters it is possible to obtain thin hot rolled strips with fine grains and appropriate texture providing satisfactory deep drawability.

#### Acknowledgements:

The authors gratefully acknowledge the financial support of this study granted by the Netherlands Institute for Materials Research (NIMR) and Hylsa, S.A. de C.V. is acknowledged for providing the material.

#### REFERENCES

- 1) L. Leduc-Lezama, M. Vazquez-del-Mercado and R. Gonzalez-de-la-Peña: *Iron Steel Eng.*, 23 (4), (1997),27.
- 2) K.W. Andrews: *J. Iron Steel Inst.*, 203, (1965), 721.
- 3) P.C. Zambrano, A.L. Delgado, M.P. Guerrero-Mata, R. Colás and L.A. Leduc: *ISIJ International* 43, (7), (2003), 1030-1035.

- 4) P.C. Zambrano, M.P. Guerrero, R. Colás and L.A. Leduc: *Mat. Char.*, 47, (2001), 275.
- 5) A.L. Delgado, Anisotropy of hot rolled low carbon steel strip, M.Eng. (Mat.) Thesis, Universidad Autónoma de Nuevo León, Mexico, (1999).
- 6) TSL<sup>®</sup> OIM Analyses for Windows: Version 3.03, (2000).
- 7) P. Van Houtte: User manual, MTM-FHM Software, Vers. 2 ed. By MTM-KU Leuven, (1995).
- 8) R.K. Ray, J. J. Jonas and R.E Hook: *Int. Mater. Rev.*, **39**, No4 (1994), 131.
- 9) R.K. Ray and J. J. Jonas: *International Materials Reviews*, **35**, No4 (1990), 6.
- 10) D. Vanderschueren, L. Kestens, P. Van Houtte, E. Aernoudt, J. Dilewijns, U.Meers: *Mater.Sci and Technology*, **6** (1990) 1247.
- 11) M.P. Butron Guillen , J.J. Jonas and R.K. Ray: *Acta met mat.*, Vol.42, No 11 (1994), 3615-3627.